Structural and electronic properties of arsenic chalcogenide molecules

Davorin Babić and Sohrab Rabii
Department of Electrical Engineering, Moore School of Electrical Engineering, and Laboratory for Research on the Structure of Matter, University of Pennsylvania, Philadelphia, Pennsylvania 19104

Jerzy Bernholc
Department of Physics, North Carolina State University, Raleigh, North Carolina 27695
(Received 17 August 1988)

Local-density cluster pseudopotential calculations have been carried out for arsenic chalcogenide molecules As_4S_4, As_4S_5, As_4S_6, and As_4Se_4. Based on the results of the calculations, a model has been developed that explains the relative stability of the arsenic sulfide molecules. Arsenic-arsenic bonds in As_4S_4 and As_4S_5 are suggested as the main reasons for the stability of these molecules. The As_4S_4 and As_4Se_4 molecules represent well the electronic properties of the corresponding solids. A randomly packed network of either As_4S_5 and As_4S_6 molecules appears to be an unlikely model for the local structure of the amorphous As_2S_3. Excellent transferability of the arsenic-sulfur bond charge density among the molecules has been found.

I. INTRODUCTION

Amorphous As chalcogenides are an interesting class of compounds since they can coexist with the crystalline forms under the same conditions. Their large photochemical sensitivity has led to applications in the field of applied optics. There is also a potential for future applications in optical computing.

Despite the abundance of experimental data on arsenic chalcogenides, the question of the local arrangement of atoms in their amorphous phase is still unresolved. Standard measurement techniques do not provide enough information to unambiguously solve this problem. Several models for the local structure have emerged in the literature, some of which are based on the gas-phase As chalcogenide molecules: As_4S_4, As_4S_5, As_4,S_6, and As_4Se_4. It is then assumed that the amorphous solid consists of random packing of these molecular units.

Even if one does not accept such a representation of the solid, an accurate description of the molecules would be very useful in its own right, as well as a test and starting point for other cluster models. Previous theoretical studies of these molecules have been listed in Ref. 1. Yamabe *et al.* have studied the As_4S_5 molecule by the semiempirical intermediate neglect of differential overlap (INDO) method.[2]

In the previous study[1] the electronic structure and properties of As_4S_4, As_4,S_6, and As_4Se_4 molecules were investigated using the self-constant-field (SCF) $X\alpha$ scattered-wave method, which employs the muffin-tin approximation for the molecular potential. While this method gives good results for certain one-electron properties, the unrealistic restrictions on the form of the potential render the calculated total energies meaningless. For the same reason the electronic charge density is not physically reliable in the interatomic region. Since most of the charge rearrangement associated with the creation of chemical bonds occurs in this region, and our goal is to understand the nature and energetics of bonding in arsenic chalcogenides, it became necessary to adopt a different approach.

The adopted method is the local-density cluster pseudopotential scheme, which has its origin in the band-structure calculations. It is first principles and, in its band-structure form, has been very successful in describing ground-state properties of solids such as binding energies, vibrational frequencies, and bond lengths. The excitation energies are considerably underestimated, but the general ordering and relative positions of the transitions are correctly described.

First-principles pseudopotentials are used to represent the effects of the nuclear potentials and the core electrons. Larger systems can now be handled because only valence electrons are explicitly treated. Application of the pseudopotentials does not involve any significant approximation to the molecular potential. One can therefore expect a reliable description of the bond charges and binding energies from the pseudopotential method.

A brief account of the theoretical techniques is given in Sec. II, and Sec. III contains the description of the results of the calculations. Measured data are compared with the calculations in Sec. IV, and Sec. V presents the conclusions.

II. THEORETICAL TECHNIQUE

The calculations are carried out within the density-functional formalism[3] using a technique developed for molecules and clusters[4] that employs the *ab initio* norm-conserving pseudopotential theory.[5] The one-electron equations solved self-consistently in the atomic units are

$$-\nabla^2\psi_i+\left[V(\mathbf{r})+\int\frac{2\rho(\mathbf{r}')}{|\mathbf{r}-\mathbf{r}'|}d\mathbf{r}'+\mu_{\rm xc}(\rho)\right]\psi_i=\varepsilon_i\psi_i\ , \quad i=1,2,\ldots,N \qquad (1)$$

where the ψ_i's represent one-electron pseudo-wave-functions and ε_i's the corresponding eigenvalues. The effective one-electron potential consists of three parts: (i) $V(\mathbf{r})$ the sum of the ionic pseudopotentials, (ii) the Coulomb repulsion potential due to the electronic charge $\rho(\mathbf{r})$, and (iii) the exchange-correlation potential $\mu_{xc}(\rho)$, which represents the effects of many-body interactions. The pseudo-charge-density is given as

$$\rho(\mathbf{r})=\sum_{i=1}^{\text{occ}} |\psi_i(\mathbf{r})|^2 . \tag{2}$$

The *ab initio* norm-conserving pseudopotentials for each atom are generated by a procedure suggested by Kerker.[6] The pseudopotentials and the pseudo-wave-functions have the property of being smooth and nodeless, and beyond a certain radius, referred to as the core radius, they match all-electron potential and wave functions, respectively. The norm-conserving property requires that the charge associated with pseudo-wave-functions and all-electron wave functions within the core radius be equal. In addition, the first and second derivatives of the all-electron wave function and pseudo-wave-function match at the core radius. By inverting the Schrödinger equation for a state with the particular energy, one gets the neutral atomic pseudopotential. The screening potential is calculated from the pseudo-charge-density as a sum of the electrostatic and exchange-correlation parts. The ionic pseudopotential is obtained by unscreening the atomic pseudopotential.

The pseudopotential is angular-momentum dependent as a result of the above requirements and constraints on the pseudo-wave-function. Its effect on a pseudo-wave-function ψ can be written as

$$V(\mathbf{r})\psi(\mathbf{r})=\sum_l V_l(\mathbf{r})P_l\psi(\mathbf{r}) , \tag{3}$$

where P_l projects the appropriate l component of the pseudo-wave-function. The nonlocality of the pseudopotential is still "weak" enough to make computations feasible.

In constructing the pseudopotential the exchange-correlation parametrization of Vosko *et al.*[7] has been used. The partial-core method[8] treats the nonlinearity of the exchange-correlation potential with respect to the valence- and core-electron interactions.

The molecular pseudopotential is a sum of the ionic pseudopotentials with no geometric restrictions on its shape. Since it is accurate outside of the region of the atomic core, it leads to a physically reliable picture of chemical bonds and related energies.

The pseudo-wave-function, pseudo-charge-density, and exchange-correlation potential of each atom are fitted to different sets of hermite Gaussian functions by a nonlinear least-squares fit. The Gaussians with the decay constants obtained by the fitting of the atomic quantities are used as computationally suitable bases for the expansion of the corresponding molecular quantities. For the molecular quantities we employ the linear least-squares fit. The fitting reduces the total number of the matrix elements from N^4 to N^3, where N is the number of basis functions. The resulting error has been carefully monitored during calculations and found to be small. The Gaussian basis sets used for the fitting consist of atom-centered functions with s, p, and d symmetry. They do not introduce appreciable geometric constraints in the fitting procedure. Table I lists the decay constants and angular symmetries for each atom.

The one-electron Schrödinger equations are thus converted to a generalized eigenvalue problem. Due to Gaussian fitting of the relevant quantities, all the matrix elements can be evaluated analytically. The use of the first-principles pseudopotentials ensures accurate treatment of the interatomic molecular potential. Furthermore, since only valence electrons enter the calculations explicitly, the total energy in the pseudopotential theory does not include the contribution of the core electrons, which is usually orders of magnitude larger than the part due to the valence electrons. Thus the variations of the total energy associated with changes of the molecular structure occupy a far larger part of the total energy and are easier to calculate.

The local-density approximation tends to overestimate the binding energy of a molecule or solid by 0.5 to 1.5 eV/atom. This is to a large part a systematic error that comes from underestimated binding energies of atoms. One should note that relative binding energies from molecule to molecule are far more accurate.

Being a ground-state theory, the local-density approach cannot reliably predict values of the optical excitation energies. However, the relative ordering and energy differences among the transitions are quite reliable.

III. RESULTS

The atomic coordinates for As_4S_4 and As_4S_6 molecules are taken from Lu and Donohue,[9] for As_4S_5 from Whitfield,[10] and for As_4Se_4 from the measurements by

TABLE I. Decay constants and angular symmetries for the Gaussian basis sets for each atom (in a.u.).

Wave function	Charge density	Exchange-correlation potential
	S	
0.085 s,p	0.2 s	0.2 s
0.25 s,p	0.4 s	0.4 s
0.8 s,r^2s,p,d	0.8 s,r^2s,p,d	0.8 s,r^2s,p,d
1.17 s,p	1.3 s	1.3 s
	2.5 s	2.5 s
	As	
0.085 s,p	0.18 s	0.132 s
0.25 s,p	0.4 s	0.36 s
0.8 s,p	0.9 s,r^2s,p,d	0.8 s
1.2 s,p	2.0 s	1.5 s,r^2s,p,d
	3.0 s	2.8 s
	Se	
0.064 s,p	0.223 s	0.078 s
0.17 s,p	0.26 s,r^2s,p,d	0.13 s,r^2s,p,d
0.45 s,p	0.375 s,r^2s,p,d	0.35 s
1.41 s,r^2s,p,d	1.5 s	0.6 s
	2.0 s	1.27 s

Goldstein and Paton.[11] Although our calculations do not use a symmetrized basis set, one should mention that As_4S_4 and As_4Se_4 molecules have D_{2d} symmetry, As_4S_6 has T_d symmetry, and As_4S_5 has no symmetry.

Table II shows the characteristic energies and electron distributions of the molecules. We have listed binding energies per atom, E_b, energies assigned to various chemical bonds, energies of the highest occupied (HOMO) and lowest unoccupied (LUMO) molecular-orbital levels, resulting optical gaps, and the atomic Mulliken populations for each type of atoms. The binding energy per atom is not a very meaningful parameter in this case since we compare molecules with different types of atoms. Since the As_4S_6 molecule has only arsenic-sulfur bonds, the As—S bond energy is evaluated by dividing the total molecular cohesive energy by 12 (number of As—S bonds). This number is then used for the arsenic-sulfur bond energy in As_4S_4 and As_4S_5. The remaining binding energy is attributed to arsenic-arsenic bonding (two As—As bonds in As_4S_4 and one in As_4S_5). The arsenic selenide molecules As_4Se_4 has two arsenic-arsenic bonds, as in As_4S_4. The length of the As—As bonds is approximately the same in both molecules. We thus assume transferability of the arsenic-arsenic bond energy, and assign the rest of its cohesive energy to eight arsenic-selenium bonds.

Comparison of the calculated binding energies in Table II with the solid-state experimental data shows good agreement. The calculated and/or estimated energy of the As—S bond is 3.5 eV, the As—Se bond 3.2 eV, and the As—As bond 4.1 and 4.5 eV. The measured energies of the arsenic-chalcogen bonds are 2.78 and 2.3 eV for crystalline As_2S_3 and As_2Se_3, respectively.[12,13] These results are consistent with the well-known overbinding of 0.5–1.5 eV produced by the local-density approximation. Antonelli *et al.*[14] have calculated the electronic structure of the crystalline As_2Se_3 and have obtained 2.5 eV/bond. The differences between their result and ours can be explained by the fact that we have made molecular calculations, whereas they have performed the calculation on an extended solid. Some of this difference may also be due to our use of a different exchange-correlation potential. The gas-phase measurement of the As—As bond[12] indicates a bond energy of 3.9 eV. This is different from our estimate of approximately 4.3 eV obtained from our As chalcogenide calculations. Such a difference should not be surprising considering that in the As_2 molecule all binding is exclusively between the two arsenic atoms, while in As_4S_4 and As_4S_5 each arsenic atom has also two sulfur bonds.

The analysis of the binding energy from molecule to molecule suggests a model for explaining the relative abundance of the As_4S_4 in the arsenic sulfide gas phase. As_4S_4 is the most closely packed of the three discussed arsenic sulfide molecules. Adding an extra sulfur atom in creating As_4S_5 breaks one arsenic-arsenic bond and pushes the arsenic atoms apart. The As atoms that formerly belonged to the broken bond are pushed far from each other, while the distance between the still-bonded arsenic atoms increases only slightly, resulting in the formation of a very strained and deformed tetrahedron. The extra sulfur atom added to form As_4S_6 breaks the remaining As—As bond and forces the arsenic atoms to move even further apart. They assume positions of an exact tetrahedron, significantly larger than the one in As_4S_4. Through all these changes the arsenic-sulfur distance has stayed approximately the same. A schematic representation of the above transformation is shown in Fig. 1.

The analysis of the valence pseudo-charge-density (Fig. 2) of arsenic-sulfur bonds in the three molecules shows excellent transferability of the bonding charge. The charge-density contours are drawn in units of 0.02 electron/bohr.[3] The atom on the right is a sulfur atom, while the two atoms on the left are As atoms. Figure 3 represents the pseudo-charge-density of arsenic-arsenic bonds in arsenic sulfide molecules. All atoms shown are arsenic atoms. The units are 0.01 electron/bohr^3. We see the existence of the As—As bond in As_4S_4 and As_4S_5, but no such bond appears in As_4S_6. In As_4S_5 two sulfur atoms are very close to the plane of the figure, resulting in a pileup of the charge in the regions marked by + signs. Similar information regarding As—As and As—Se bonds in the As_4Se_4 molecule is shown in Fig. 4. The As—As bond in As_4Se_4 is very similar to the corresponding bond in As_4S_4. As expected, there are differences between the As—Se and As—S bond pseudo-charge-density in As_4X_4 molecules. Comparing the contours from Figs. 2–4 with the appropriate figures in Ref. 1, we notice that

TABLE II. Characteristic energies and atomic Mulliken populations of the As chalcogenide molecules. E_b is the binding energy, E's are the bond energies, and Q's are the atomic Mulliken populations.

Molecule	As_4S_6	As_4S_5	As_4S_4	As_4Se_4
E_b/atom (eV)	4.23	4.42	4.56	4.18
E(As—S) (eV)	3.53	3.53	3.53	
E(As—As) (eV)		4.52	4.13	4.13
E(As—Se) (eV)				3.15
E_{HOMO} (eV)	−5.56	−6.03	−5.90	−5.17
E_{LUMO} (eV)	−4.21	−3.90	−2.98	−3.45
E_g (eV)	1.35	2.13	2.92	1.72
Q(As) (electron)	4.77	4.60 (av)	4.65	4.94
Q(S or Se) (electron)	6.15	6.32 (av)	6.35	6.06

there is more valence charge in the interatomic region in the pseudopotential case than in the scattered-wave calculation. The directionality of the chemical bonds is also more pronounced. We believe that the valence charge obtained through the use of pseudopotentials is more accurate since it does not employ the muffin-tin approximation in the most sensitive interstitial region.

Figure 5 represents the energy-level diagram for the molecules, together with the Mulliken populations[15] per atom for each level, except for As_4S_5, where we show the sum of the atomic populations over all atoms of the same kind. These energy levels should be compared with the atomic valence levels calculated using the same pseudopotential: -17.1 eV for the s and -7.2 eV for the p level of sulfur, -14.1 and -5.3 eV for arsenic, and -16.9 and -6.6 eV for selenium. The levels that are extended over different types of atoms are clearly noticeable. The detailed analysis of the populations shows marked separation of the levels originating from s and p atomic orbitals, although most "p" levels have from 1% to 8% s com-

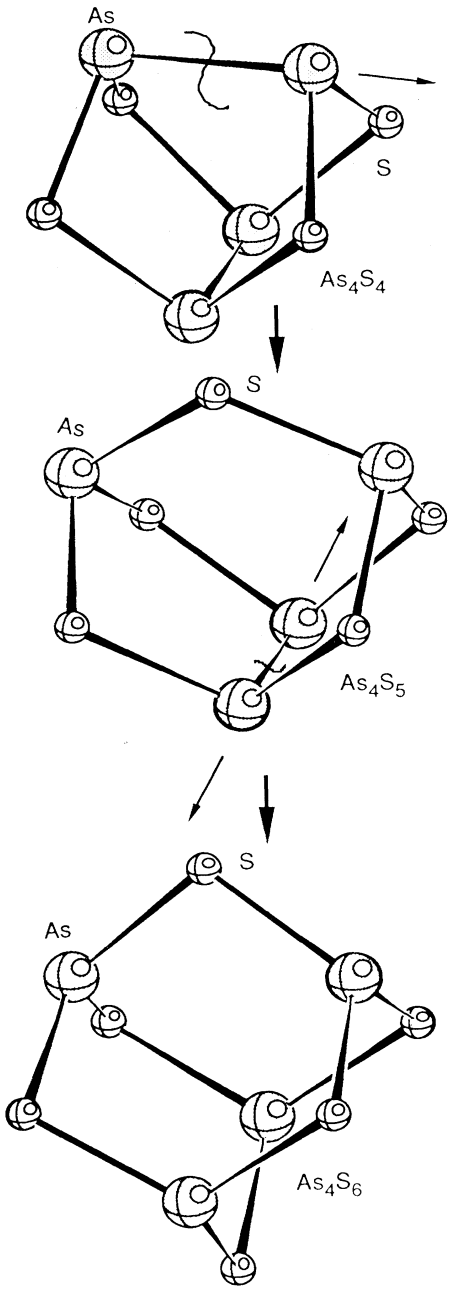

FIG. 1. Schematic representation of the transformations involved in the formation of the arsenic sulfide molecules.

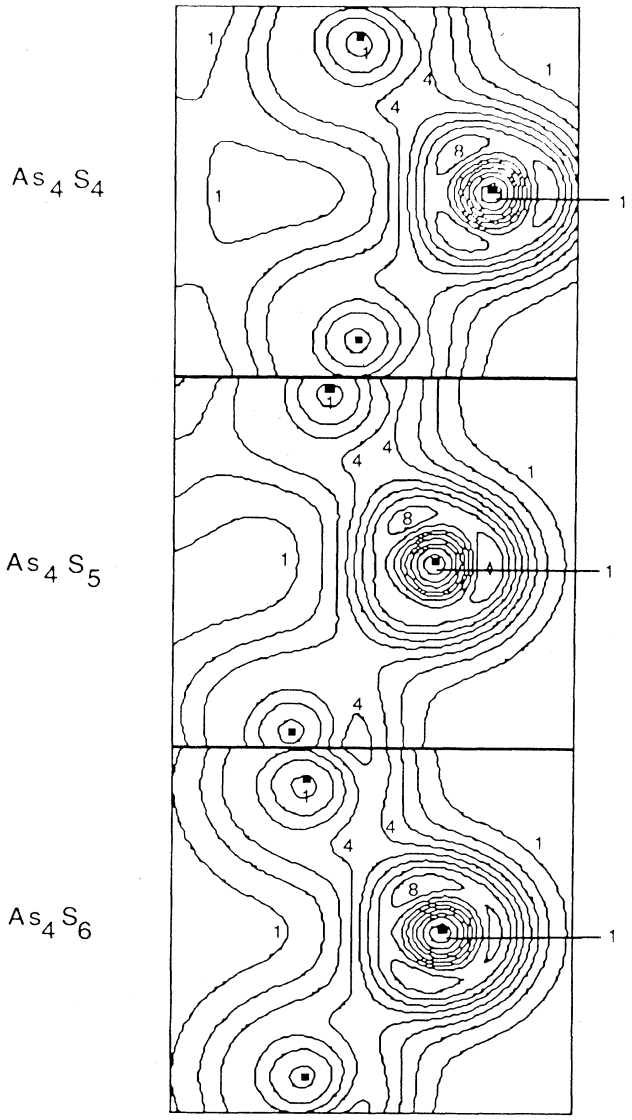

FIG. 2. Valence charge-density contours of the arsenic-sulfur bonds for the arsenic sulfide molecules in units of 0.02 electron/bohr^3. The pairs of atoms on the left are arsenic atoms, whereas the single atoms on the right are sulfur atoms.

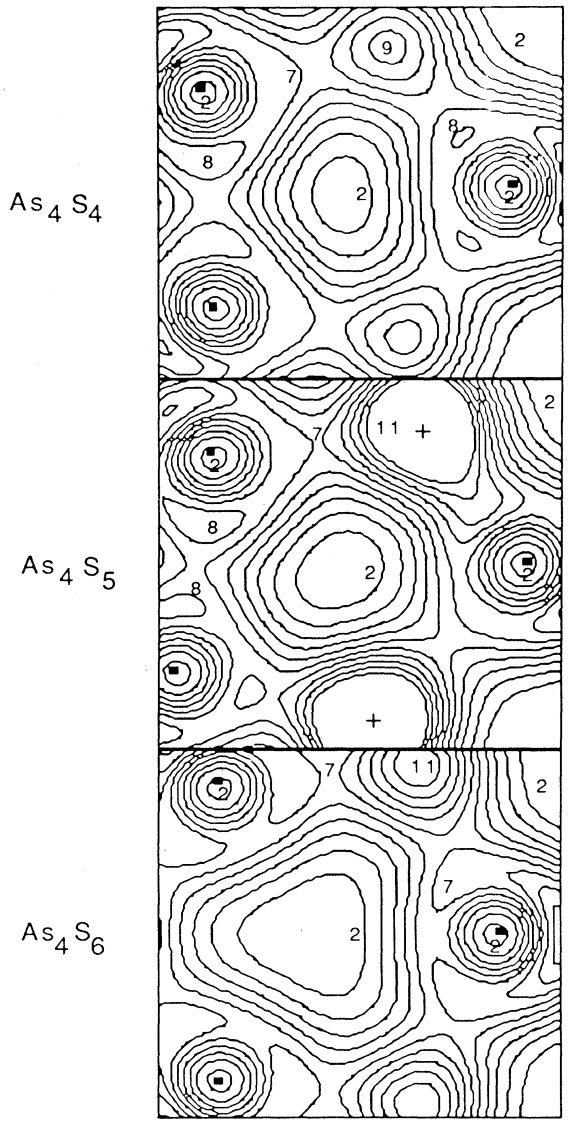

FIG. 3. Valence charge-density contours in the arsenic plane of the arsenic sulfide molecules in units of 0.01 electron/bohr^3. All the atoms shown are arsenic atoms.

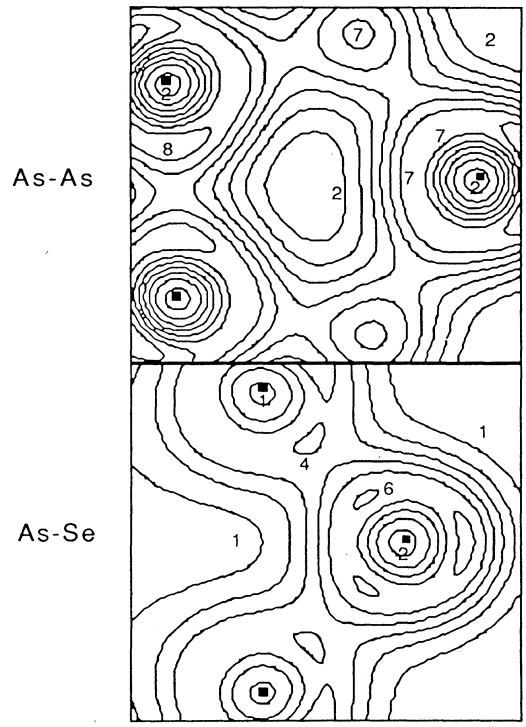

FIG. 4. Valence charge-density contours for the arsenic-arsenic and arsenic-chalcogen bonds in the As_4Se_4 molecule. The units and the other details are the same as for corresponding contour plots in Figs. 2 and 3.

ponents. The molecular "*s*" levels are in the range from -22 to -13 eV, while "*p*" levels are situated from -11 eV up. In As_4S_4, As_4Se_4, and As_4S_6 all atoms of one kind are symmetry equivalent. The HOMO's of both As_4X_4 molecules are chalcogen *p* lone pairs, while LUMO's are As-chalcogen *p* hybridized. For As_4S_6, HOMO's and LUMO's are strongly arsenic-sulfur–hybridized, predominantly *p*-type levels. Due to its lack of symmetry, As_4S_5 is a special case: no atoms are symmetry equivalent to each other. The atomic Mulliken populations vary 3% for arsenic atoms and less than 1% for sulfur atoms in this molecule. Its HOMO is predominantly sulfur *p*, whereas its LUMO is arsenic *p* with some *s* contribution. Comparing the atomic populations in As_4S_4 and As_4S_6, we see greater ionic character of the bonds in As_4S_4 than in As_4S_6. Since the arsenic-sulfur bond length does not change appreciably in all these molecules, the overlap of the atomic pseudo-wave-functions that controls the covalent bonding and its strength is expected to remain constant from molecule to molecule. The increased ionic character of the bonds in As_4S_4 can therefore provide an additional contribution to its stability. Turning to As_4Se_4, the As—Se bond is almost homopolar, the Mulliken charge transfer being only 1%. This is due to the fact that arsenic and selenium are neighbors in the Periodic Table.

We have also calculated the equilibrium length of the arsenic-sulfur bond in As_4S_4 and As_4S_6 and the arsenic-arsenic bond in As_4S_4. For each type of bond the total energy was calculated by varying the bond length along the bond direction while all the other bond lengths and the symmetry of the molecule were kept constant. To achieve this, the bond angles had to be allowed to vary in the process. The resulting sets of bond lengths and total energies were fitted to the Morse equation. This approach was chosen as the most suitable to calculate the vibrational frequencies associated with each bond. Table III shows the parameters of the fits and the values of the equilibrium bond lengths. The experimental length of the arsenic-sulfur bond is in the range of 2.23–2.25 Å.[9–11] We obtain this value to within 5%. However, this is not good enough to calculate the vibrational frequencies asso-

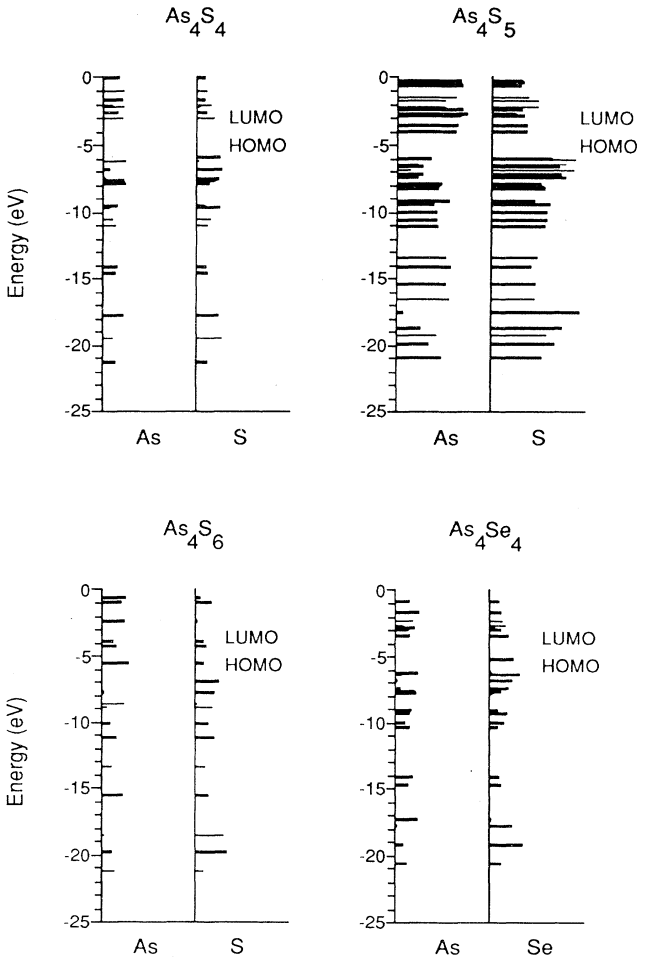

FIG. 5. Energy-level diagrams and Mulliken populations for each molecule. The length of the lines in the panel is proportional to the Mulliken population of the levels.

ciated with the bonds. The vibrational frequencies are related to the second derivatives of the cohesive energy with respect to the bond length and are, therefore, very sensitive to any errors in the form of the cohesive energy function. A possible source of our problem can be that we do not use d-type Gaussian functions in the expansion of the arsenic atomic orbitals. This might have made our basis set incomplete to calculate accurately the changes in the molecular binding energy produced by the variations of the bond lengths. We believe that the inclusion of the bond-bending forces is necessary to obtain an improved description of the equilibrium bond lengths and vibrational frequencies. We also believe that a better value for the equilibrium bond lengths could have been found if the total energies were minimized with respect to uniform contraction and expansion of the molecules.

TABLE III. Coefficients for the Morse fit to the variations of the total energy with respect to the characteristic bond lengths for As_4S_4 and As_4S_6.

Bond:	As—As	As—S	As—S
Molecule:	As_4S_4	As_4S_4	As_4S_6
b_1 (Ry)	2.69	2.90	3.17
b_2 (Å^{-1})	0.56	2.17	1.81
$r_0=b_3$ (Å)	2.58	2.35	2.17
b_4 (Ry)	−190.80	−191.00	−241.32
r_0 (Å) (expt)	2.49	2.23	2.25

IV. COMPARISON WITH EXPERIMENT

Figure 6 shows the comparison of the calculated density of valence states for each molecule with the measured x-ray-photoemission (XPS) spectra for the corresponding amorphous solid. The theoretical curve is labeled I and is obtained by Gaussian broadening of the valence states. To account for the effect of the shorter lifetimes of the deeper holes on the measured spectra, we have employed energy-dependent broadening,

$$\sigma(E)=a+b|E-E_{\mathrm{HOMO}}| \ .$$

The linear expression is used based on the measured inverse lifetimes of the holes in the simple metals.[16] We are not aware of any such scheme or data dealing with covalent semiconductors. The coefficients in the broadening expression are chosen to obtain the best agreement with the measured data. Their values are $a=0.25$ eV and $b=0.10$ eV for As_4S_4 and As_4Se_4, and $a=0.35$ eV and $b=0.02$ eV for As_4S_5 and As_4S_6.

The curves labeled II in Fig. 6 are taken from the experimental part of the work by Salaneck *et al.*[17] on solid As_4S_4 and As_4Se_4, the curves labeled III by Takahashi

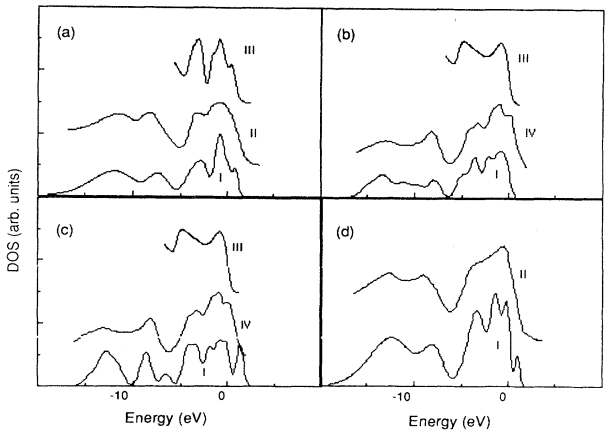

FIG. 6. Comparison of theoretical density of states for each molecule with different experimental XPS spectra measured on the corresponding amorphous solids. (a) As_4S_4 molecule with As_4S_4 solid; (b) As_4S_5 molecule with As_2S_3 solid; (c) As_4S_6 molecule with As_2S_3 solid; (d) As_4Se_4 molecule with As_4Se_4 solid. Curve I is the theoretical curve. Curves II, III, and IV are from Refs. 17, 18, and 19, respectively.

and Harada[18] have been measured on vapor-deposited films of As_2S_3 and As_4S_4, while curve IV has been measured on an amorphous thin film of As_2S_3.[19] We emphasize that the theoretical data for both As_4S_5 and As_4S_6 molecules are compared with the experiment data obtained on the amorphous As_2S_3 solid. All the curves have been aligned to get the best overall agreement.

In the case of the molecular solids As_4S_4 and As_4Se_4, where the electronic structure of one molecule is expected to represent well that of the extended solid, we have excellent agreement between theory and experiment. All features of the experimental XPS spectra are faithfully reproduced. The agreement between the experimental and theoretical data in the case of As_4S_5 and As_4S_6 molecules is also very good, except for the highest-energy peak in the density of states of As_4S_6. The theoretical spectrum in this region contains both more structure and sharper peaks than the experimental data. The sharpness of the highest-energy peak in the calculated spectrum is caused by the degeneracy of the molecule's HOMO due to high symmetry. The next lower molecular level is a full 1.2 eV below the HOMO. Such a high symmetry does not exist in the amorphous solid, and the levels of the solid are spread out in energy. If we choose a broadening large enough to create a significant overlap of the As_4S_6 molecule's HOMO and its next lower level, other prominent features of the calculated spectrum will be destroyed. As_4S_5 has no symmetry, but has one arsenic-arsenic bond. Lack of such a bond in the As_2S_3 amorphous solid rules out that glassy As_2S_3 consits of randomly packed As_4S_5 molecules.

The local-density approximation underestimates the value of the optical gap up to 50%. Our calculated values for the optical gap, listed in Table II, fall within the range of expected error since the measured gaps for glassy As_2S_3 and As_2Se_3 are ~ 2.36 and ~ 1.76 eV, respectively.[20] The large gaps obtained for the As_4X_4 molecules are caused by the smallness of these molecules. In comparison to the solids, these effects compensate for the effects of the local-density approximation.

V. DISCUSSION AND CONCLUSIONS

Based on the analysis of the cohesive energies and bond-charge densities, we have developed a model for the stability of arsenic sulfide molecules. The As_4S_4 molecule is closed packed and has two arsenic-arsenic bonds. Addition of extra sulfur atoms to create the As_4S_5 and As_4S_6 molecules breaks As—As bonds and pushes arsenic atoms away from each other. The arsenic-sulfur bond length stays approximately the same. The final As_4S_6 molecule has a far more open structure than the As_4S_4 molecule. Since the arsenic-arsenic bonds are ~ 0.5 eV stronger than the arsenic-sulfur bonds in the As sulfide molecules, the breaking of As—As bonds decrease the stability of the molecules. Therefore, the As_4S_4 molecule is the most stable, while the As_4S_6 is the least stable of the set. This explains the abundance of the As_4S_4 component in the mass spectra of arsenic sulfides.

The As_4X_4 molecules are good models for the corresponding solids based on the excellent agreement between the calculated density of states and the XPS spectra. However, the amorphous As_2S_3 cannot be considered as a randomly packed network of any of the molecules studied. The As_4S_6 molecule has only arsenic-sulfur bonds, similar to the glassy As_2S_3, but its local symmetry is too high compared to the solid. This would be reflected in, for example, XPS spectra of the solid. The arsenic-arsenic bonds are essential for the stability of the As_4S_4 and As_4S_5 molecules and, again, would be seen as a strong feature in the solid's XPS spectra. Since there is no evidence for such prominent As—As bonding in the As_2S_3 amorphous solid, these molecules appear to be unlikely models for the solid's local structure. The results are not consistent with the structural models of the amorphous As_2S_3 suggested by several workers.[21–23]

The arsenic-sulfur bond-charge density is shown to be transferable between different molecules. The bond lengths and energies are in agreement with the experimental data.

ACKNOWLEDGMENTS

The authors would like to acknowledge Professor S. G. Louie, Professor E. J. Mele, and Professor E. W. Plummer for helpful discussions. This work was supported in part by the U.S. National Science Foundation/ Laboratory for Research on the Structure of Matter under Grant No. DMR-85-19059 and by the U.S. Air Force Office of Scientific Research under Grant No. AFOSR-84-0320.

[1]D. Babić and S. Rabii, Phys. Rev. B **38**, 10 490 (1988).
[2]T. Yamabe, K. Tanaka, A. Tachibana, Y. Kobayashi, H. Teramae, and K. Fukui, Solid State Commun. **40**, 521 (1981).
[3]P. Hohenberg and W. Kohn, Phys. Rev. **136**, B864 (1984); W. Kohn and L. J. Sham, *ibid.* **140**, A1133 (1965).
[4]J. Bernholc and N. A. W. Holzwarth, Phys. Rev. Lett. **50**, 1451 (1983); J. Chem. Phys. **81**, 3987 (1984).
[5]D. R. Hamann, M. Schlüter, and C. Chiang, Phys. Rev. Lett. **43**, 1494 (1979).
[6]G. Kerker, J. Phys. C **13**, L189 (1980).
[7]S. H. Vosko, L. Wilk, and M. Nusair, Can. J. Phys. **58**, 1200 (1980).
[8]S. G. Louie, S. Froyen, and M. L. Cohen, Phys. Rev. B **26**, 1738 (1982).
[9]C. S. Lu and J. Donohue, J. Am. Chem. Soc. **66**, 818 (1944).
[10]H. J. Whitfield, J. Chem. Soc. Dalton Trans. **12**, 1740 (1973).
[11]P. Goldstein and A. Paton, Acta Crystallogr. Sect. B **30**, 915 (1974).
[12]The National Bureau of Standards Tables of Chemical Thermodynamic Properties, in J. Phys. Chem. Ref. Data **11**, Suppl. No. 2 (1982).
[13]M. B. Myers and E. J. Felty, J. Electrochem. Soc. **117**, 818 (1970).
[14]A. Antonelli, E. Tarnow, and J. D. Joannopoulos, Phys. Rev.

B **33**, 2968 (1986).
[15]R. S. Mulliken, J. Chem. Phys. **23**, 1833 (1955).
[16]E. W. Plummer, Surf. Sci. **152-153**, 162 (1985), and private communication.
[17]W. R. Salaneck, K. S. Liang, A. Paton, and N. O. Lipari, Phys. Rev. B **12**, 725 (1975).
[18]T. Takahashi and Y. Harada, Solid State Commun. **35**, 191 (1980).
[19]W. R. Salaneck and R. Zallen, Solid State Commun. **20**, 793 (1976).
[20]N. F. Mott and E. A. Davis, *Electronic Processes, in Non-Crystalline Materials* (Clarendon, Oxford, 1979), pp. 500 and 501.
[21]J. P. DeNeufville, S. C. Moss, and S. R. Ovshinsky, J. Non-Cryst. Solids **13**, 191 (1973/74).
[22]R. J. Nemanich, G. A. N. Connell, T. M. Hayes, and R. A. Street, Phys. Rev. B **18**, 6900 (1978).
[23]M. F. Daniel, A. J. Leadbetter, A. C. Wright, and R. N. Sinclair, J. Non-Cryst. Solids **31**, 271 (1979).